



Identification of *ACSL4* as a biomarker and contributor of ferroptosis in clear cell renal cell carcinoma

Na Guo^{1,2}

¹Department of Anesthesiology, Sun Yat-sen University Cancer Center, State Key Laboratory of Oncology in South China, Collaborative Innovation Center for Cancer Medicine, Guangzhou, China; ²Guangdong Esophageal Cancer Institute, Guangzhou, China

Correspondence to: Na Guo. 651 Dongfeng Road East, Guangzhou 510060, China. Email: guona@sysucc.org.cn.

Background: Acyl-CoA synthetase long-chain family member 4 (*ACSL4*) has been linked to the ferroptosis process and is implicated in the pathogenesis of tumors. Nevertheless, neither the expression levels of *ACSL4* nor its prognostic significance in clear cell renal cell carcinoma (ccRCC) is completely understood at this time.

Methods: Predictions of the *ACSL4* mRNA expression in ccRCC and its link to ccRCC prognosis were made based on data from the Oncomine and The Cancer Genome Atlas (TCGA) databases. Through the use of real-time polymerase chain reaction (PCR), we ascertained the levels of *ACSL4* expression in human RCC samples. Analyses of the link between *ACSL4* expression and the survival of ccRCC patients were undertaken using the Kaplan-Meier (KM) plotter database. To study the function that *ACSL4* plays in ferroptosis in ccRCC cell lines, either upregulation or knockdown of its expression was performed.

Results: We found that the *ACSL4* expression level was considerably down-modulated in ccRCC samples ($P < 0.001$), which was in line with the analytical results of the Oncomine and TCGA database. The subsequent immunohistochemistry findings revealed that *ACSL4* levels in ccRCC samples were much lower or not undetectable in contrast with those in normal samples. The level of differential *ACSL4* expression was strongly associated with factors such as disease stages, gender, tumor grade, nodal invasion, and ccRCC subtypes (all $P < 0.001$). According to the results of the survival analysis, the overall survival was satisfactory among ccRCC patients who had overexpressed *ACSL4* ($P = 0.014$). In cancer cells, ferroptosis sensitization may be restored by overexpressing *ACSL4* via the process of transfection; however, increasing ferroptosis resistance can be achieved by suppressing *ACSL4* expression through the use of shRNA. Protein ubiquitination could have a function in influencing the way that *ACSL4*-induced ferroptosis works mechanically.

Conclusions: *ACSL4*, which is a mediator and monitor of ferroptosis, was lowered in expression in ccRCC and acted as a valuable diagnostic and prognostic biological marker, thus representing a novel promising treatment target for ccRCC.

Keywords: Acyl-CoA synthetase long-chain family member 4 (*ACSL4*); biomarker; ferroptosis; clear cell renal cell carcinoma (ccRCC)

Submitted Oct 05, 2021. Accepted for publication Jun 05, 2022.

doi: 10.21037/tcr-21-2157

View this article at: <https://dx.doi.org/10.21037/tcr-21-2157>

Introduction

Renal cell carcinoma (RCC), which is among the most prevalent malignancy affecting the urinary tract, is attributed to 2–3 percent of all cancers that occur in adults.

Clear cell renal cell carcinoma (ccRCC), which is the most prevalent type of RCC, is typically characterized by an elevated metastatic risk and unfavorable responsiveness to radiation and chemotherapy (1,2). It is important to highlight that 30% of individuals with ccRCC experienced

localized advancement and distant metastases when they are being diagnostically identified, and this is the major cause of the increased fatality rates for these patients (3). Consequently, it is beneficial to create diagnosis and therapy targets by identifying genes that have varying levels of expression in ccRCC.

Acyl-CoA synthetase long-chain family member 4 (*ACSL4*), which is often referred to as *FACL4*, was found in the year 2002 as the mutant gene attributed to the non-specific X-linked mental retardation (4). According to the findings of Maloberti and his colleagues, *ACSL4* has a substrate selectivity for arachidonic acid (AA) as well as eicosapentaenoic acid (EPA). Even more intriguing is the observation that the levels of free AA may, in turn, influence the levels of the *ACSL4* protein inside the cells (5). To this point, it has been demonstrated that dysregulation of *ACSL4* is associated with a significant variety of disorders, some of which include diabetes (6), acute kidney injury (7), and malignant tumors (8).

Cancer cells often exhibit either innate or acquired resistance to the programmed cell death process known as apoptosis. As a consequence, the generation of non-apoptotic types of controlled cell death has emerged as a promising therapeutic technique for treating cancers (9). The newly identified, non-apoptotic, controlled cell death known as ferroptosis was found for the first time in cancerous cells with an oncogenic *Ras* mutation (10). In recent research, it was shown that silencing *ACSL4* prevented erastin from inducing ferroptosis in HL60 and HepG2 cells, and that overexpressing *ACSL4* reverted K562 and LNCaP cells back to their previous levels of sensitivity to the ferroptosis mediator erastin (11). The lowered *ACSL4* expression level, which anticipates a cell line's susceptibility to ferroptosis, may be found in a variety of RCC cell lines (12). As a result, the levels of *ACSL4* expression could be connected to the advancement of ccRCC because of the role it plays in inducing ferroptosis. Nonetheless, neither the expression patterns nor the functional relevance of *ACSL4* in ccRCC has been investigated to this point. In light of this, the current work evaluated the expression *ACSL4* in ccRCC as well as its correlations with patients' clinical and pathological variables and prognoses. Additionally, the impact of *ACSL4* on ferroptosis was explored by undertaking experimental and bioinformatics studies. I present the following article in accordance with the REMARK reporting checklist (available at <https://tcr.amegroups.com/article/view/10.21037/tcr-21-2157/rc>).

Methods

Analysis of ACSL4 using bioinformatics

To determine the expression levels of *ACSL4* mRNA in ccRCC and corresponding normal samples, we employed the OncoPrint database (<https://www.oncoPrint.org>) (13), including Beroukhim Renal dataset, Lenburg renal datasets, Gumz Renal and Jones Renal datasets. Subsequently, we screened The Cancer Genome Atlas (TCGA) KIRC database to determine the link between *ACSL4* mRNA expression and ccRCC patients' prognoses from UALCAN (<http://ualcan.path.uab.edu>) (14). In The Human Protein Atlas (HPA) (<https://www.proteinatlas.org>) (15), immunohistochemical imaging (Antibody HPA005552) was utilized to undertake a comparative assessment of the expression levels of *ACSL4* protein found in human ccRCC and normal samples. Utilizing a web-based database named Kaplan-Meier (KM) Plotter (<https://kmplot.com>), we investigated the potential prognostic significance of overexpressed *ACSL4* (16). The KM Plotter dataset contains an analysis of tumor mutation burden (TMB), which is described as the actual number of indel mutations per million bases, base substitutions, and somatic coding errors. This analysis provides an accurate assessment of both the total neoantigen load as well as the mutational load. All samples were divided into high and low tumor mutation burden groups with median value as the cutoff point. cBioPortal (<http://www.cbioportal.org>) was utilized to conduct a study of *ACSL4* gene expression based on the TCGA-KIRC dataset (17). Functional analyses of *ACSL4* were conducted by Gene Ontology (GO) and Kyoto Encyclopedia of Genes and Genomes (KEGG) in the Database for Annotation, Visualization, and Integrated Discovery (DAVID) (<https://david.ncifcrf.gov/summary.jsp>) (18). The ccA and ccB molecular subtypes of RCC are defined as previous research reported (2).

Specimens of human ccRCC tissue

In total, this research comprised 16 participants who received ccRCC diagnoses at the cancer center of Sun Yat-sen University between the years 2018 and 2019. The cancer samples of these patients, together with 5 cm of adjoining non-tumor tissues, were taken for further qPCR testing. Prior to undergoing a surgical operation, these patients did not receive any adjuvant treatment, including radiation, chemotherapy, or any other kind of treatment. The study was conducted in accordance with

the Declaration of Helsinki (as revised in 2013). This study was approved by the Academic Committee of Sun Yat-sen University Cancer Center (No. B2018-006-01), and informed consent was taken from all the patients.

Cell culture

The American Type Culture Collection (ATCC, Manassas, VA, USA) supplied all four of the ccRCC cell lines that were used in this study: RCC4, A498, 769-P, and 786-O. We cultured the cells in a humid chamber at 37 °C comprising 5% carbon dioxide utilizing a DMEM high glucose medium supplemented with 10% fetal bovine serum (FBS) and 100 U/mL of streptomycin/penicillin.

Cell proliferation

The Cell Counting Kit-8 (CCK-8) experiment was undertaken to ascertain the proliferative capacity of cells in compliance with the specifications provided by the manufacturer.

Western blotting assays

Lysis of the samples or cells was achieved utilizing RIPA buffer, and the BCA kit (Beyotime Institute of Biotechnology, Shanghai, China) was adopted to quantify the protein concentration. SDS-PAGE was performed on 30 µg total proteins derived from the cells or tissues, after which they were deposited into a PVDF membrane (Millipore, Bedford, MA, USA). After being blocked with skim milk at a concentration of 5% for one hour at ambient temperature, the PVDF membranes were subjected to overnight incubation in a primary antibody at 4 °C. The next step involved rinsing the membranes thrice using PBST and subsequently incubating them for 2 h at ambient temperature with a secondary antibody. Eventually, visualization of the signals was done with exposure to X-ray films and super or enhanced chemiluminescence (Pierce, Rockford, IL, USA).

Quantitative real-time polymerase chain reaction (qPCR) analysis

Synthesis of first-strand cDNA was accomplished with the aid of the Reverse Transcription System Kit (OriGene Technologies) following the guidelines stipulated by the manufacturer. cDNA obtained from the cell specimens

was amplified utilizing appropriate primers (*ACSL4*: 5'-AGGTGCTCCAACCTCTGCCAGTA-3' and 5'-GCTATCTCCTCAGACACACCGA-3') and the results were standardized with respect to actin RNA (5'-AGGTCTTTGCGGATGTCCACGT-3' and 5'-CACCATTGGCAATGAGCGGTTTC-3').

RNAi and gene transfection

Sigma Aldrich (St. Louis, MO, USA) was the supplier for the human *ACSL4*-shRNA. OriGene Technologies supplied the human *ACSL4*-cDNA. The Lipofectamine™ 3000 or Lentivirus Transduction System was utilized to carry out the transfections in line with the specifications provided by the manufacturer.

Iron assay

The level of ferrous iron (Fe²⁺) contained inside cells or within mitochondria was measured with an iron assay kit obtained from Sigma Aldrich following the requirements stipulated by the manufacturer.

Lipid ROS assays

After being treated in the manner specified, the cells were subjected to trypsinization and resuspension in a medium that contained 10% FBS to perform a lipid ROS assay. After that, 10 µM of C11-BODIPY (Thermo Fisher, Waltham, MA, USA) was introduced into the specimens, which were subsequently incubated for 30 minutes at 37 °C with 5% carbon dioxide while being shielded from light. To get rid of any residual C11-BODIPY, the cells were rinsed twice in PBS. By utilizing a flow cytometer, we assessed the fluorescence of C11-BODIPY (581/591) by simultaneously collecting red (581/610 nm) and green (484/510 nm) signals at different wavelengths.

Statistical analysis

GraphPad Prism 6.0 (GraphPad Software, San Diego, CA, USA) and SPSS 22.0 (IBM SPSS, Chicago, IL, USA) were utilized to execute all analyses of statistical data. The results from the statistical analysis were presented as means ± SD. The two-tailed Student's *t*-test and the ANOVA LSD test were implemented to assess whether there was a significant difference across the subgroups. The threshold for statistical significance was determined to be P value <0.05.

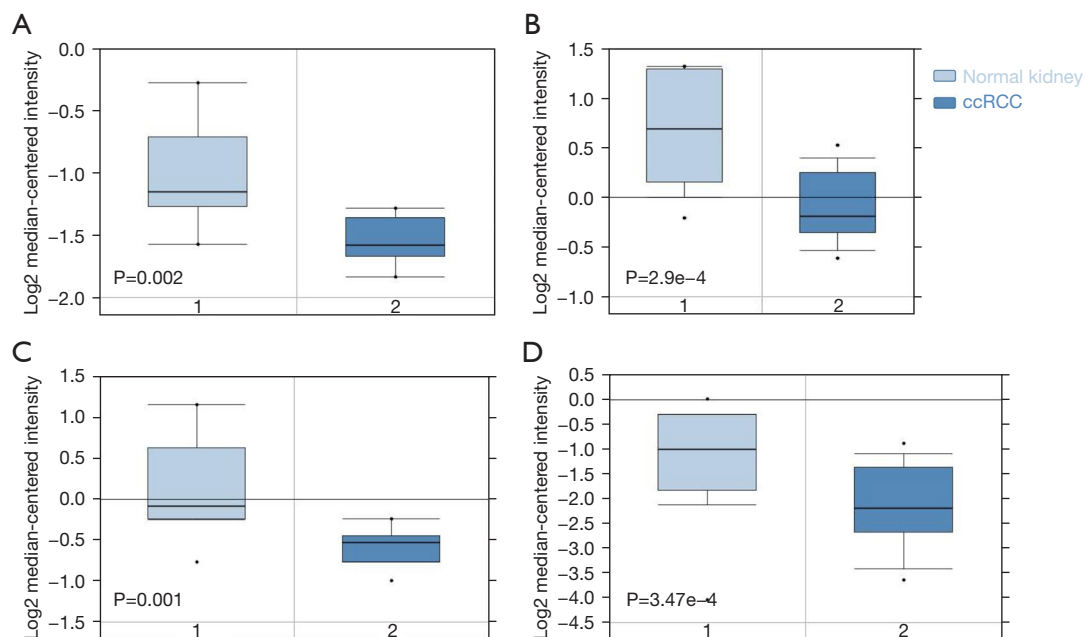


Figure 1 Low expression levels of *ACSL4* mRNA in ccRCC predicted by the Oncomine database. The Oncomine database mining analysis of *ACSL4* mRNA levels in (A) Lenburg Renal, (B) Beroukhim Renal, (C) Gumz Renal, and (D) Jones Renal grouped by ccRCC and normal kidney. ccRCC, clear cell renal cell carcinoma.

Results

Expression of ACSL4 is down-modulated in ccRCC

Premised on the analysis of the Oncomine database, we discovered that the level of *ACSL4* mRNA expression was considerably lower in ccRCC in contrast with the normal samples (*Figure 1*). The use of qPCR allowed for the detection of *ACSL4* expression in postoperative ccRCC tumor samples relative to normal kidney samples. When tumor tissues (n=16) were subjected to a comparison with their matched normal tissues (n=16), the relative *ACSL4* expression level was found to be considerably lower in the former (P<0.001, *Figure 2A*). Following that, we examined the HPA database to find evidence of the *ACSL4* protein expression. It was shown that *ACSL4* IHC is expressed partly in some tubules in normal kidney with moderate to high staining (*Figure 2B*). The percentage of samples with positive *ACSL4* expression was 72.7 percent (8/11 samples). In contrast, nearly no or extremely weak *ACSL4* staining was found in the majority of tumor samples, and staining was mostly distributed on the cytoplasm and the cell membrane (*Figure 2C,2D*).

Decreased ACSL4 mRNA expression is linked to malignant clinical-pathological characteristics in ccRCC patients

We additionally evaluated the association of *ACSL4* mRNA expression with clinical and pathological characteristics based on the UALCAN data set. These results showed the level of *ACSL4* mRNA was considerably lowered in the ccRCC group in contrast with the normal group (*Figure 3A*, P<0.001), despite cancer stages, tumor grade, nodal invasion, ccRCC subtypes, or gender (*Figure 3B-3F*). By employing the survival data retrieved from the KM plotter, we plotted KM curves of RFS (relapse-free survival) and OS (overall survival) based on data from 530 patients (including 195 *ACSL4* low expression patients and 335 *ACSL4* high expression cases) to examine the relationship of mRNA expression of *ACSL4* with ccRCC patients' prognoses. According to the findings, patients who had upregulated *ACSL4* exhibited remarkably longer OS time (P=0.014; *Figure 4A*). In terms of RFS, higher expression of *ACSL4* was also related to better survival, but it is not statistically significant (P=0.29; *Figure 4B*). Additional subgroup

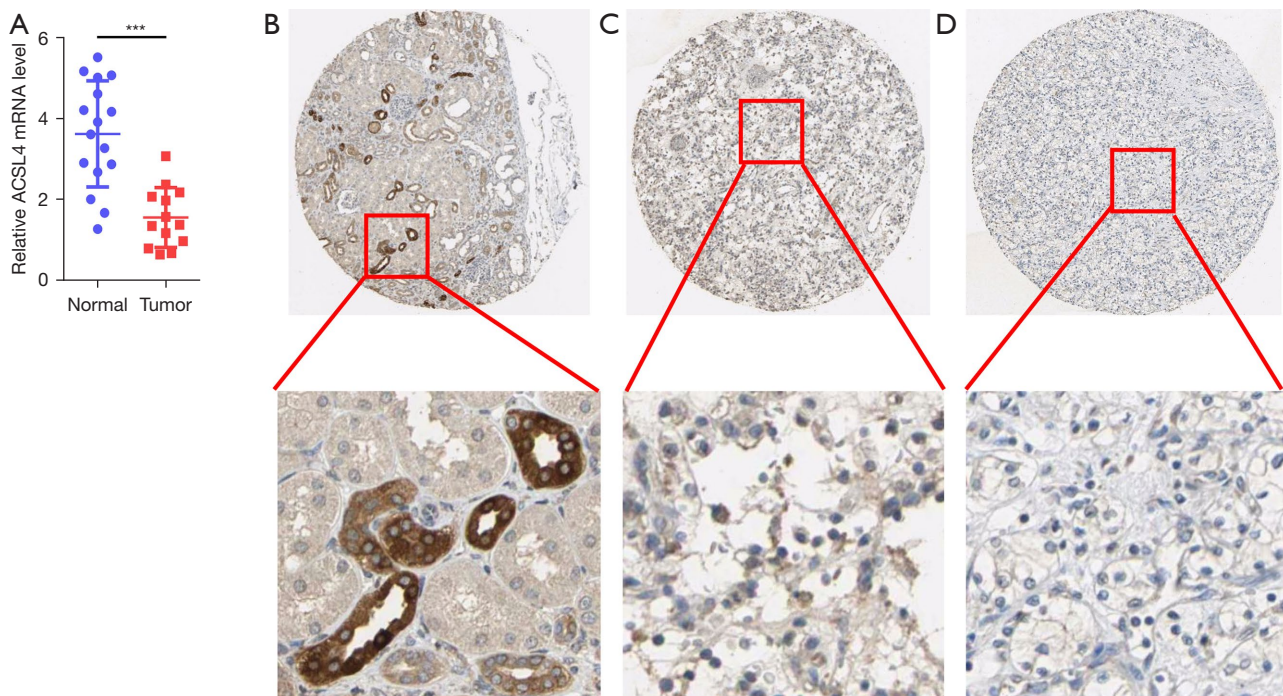


Figure 2 *ACSL4* was significantly down-regulated in ccRCC tissues compared with normal kidney tissues. (A) *ACSL4* mRNA expression was analyzed by qPCR in 16 pairs of ccRCC tissues and matched adjacent normal kidney tissues. (B) *ACSL4* immunohistochemistry showed medium staining in normal kidney tissue; (C) low staining in ccRCC tissue; (D) not detected staining in ccRCC tissue. The top is magnified $\times 50$, the below is magnified $\times 200$. ***, $P < 0.001$. ccRCC, clear cell renal cell carcinoma.

analyses illustrated favorable OS with higher *ACSL4* expression for female patients ($P = 0.013$; *Figure 4C*), those with a more advanced grade and stage of the tumor ($P = 0.046$ and $P = 0.13$, correspondingly; *Figure 4D, 4E*), and those with TMB ($P = 0.013$; *Figure 4F*).

ACSL4 upregulation enhances ferroptosis

To verify our hypotheses that the *ACSL4* dysregulation was associated with ferroptosis in ccRCC, we measured *ACSL4* expression in 4 renal cancer cells. RCC4 and A498 cells expressed relatively elevated levels of *ACSL4*, in contrast with 769-P and 786-O cells, which expressed extremely low levels (*Figure 5A*). Next, we explored whether or not the *ACSL4* expression is responsible for erastin's anticancer effect (a ferroptosis inducer). The transfection of *ACSL4* cDNA into 769-P and 786-O cells resulted in the upregulation of the mRNA levels of *ACSL4* (*Figure 5B*). Upregulation of *ACSL4* expression mediated by gene transfection greatly enhanced the susceptibility of 769-P and 786-O cells to the erastin-mediated cell death (*Figure 5C, 5D*), providing

further evidence for the hypothesis that *ACSL4* functions as a positive modulator of ferroptosis. Both lipid peroxidation and the buildup of ferrous ion (Fe^{2+}) are necessary steps in the process of ferroptosis induction. As a consequence, we investigated whether or not *ACSL4* affected these events during ferroptosis. Notably, erastin-mediated lipid ROS generation was considerably enhanced by the upregulation of *ACSL4* (*Figure 5E*). Conversely, erastin-mediated Fe^{2+} levels were not influenced by the *ACSL4* upregulation (*Figure 5F*), indicating that *ACSL4* modulates the cellular lipid composition rather than iron accumulation. The results above showed that *ACSL4* leads to a decrease in cell number and overload of lipid peroxidation, all of which may partially result in ferroptosis of ccRCC cells.

ACSL4 knockdown suppresses ferroptosis

To additionally validate the function of *ACSL4* in ferroptosis, we transfected a selective shRNA targeting *ACSL4* into RCC4 and A498 cell lines, which resulted in a considerable reduction in the levels of *ACSL4* mRNA (*Figure 6A*). The

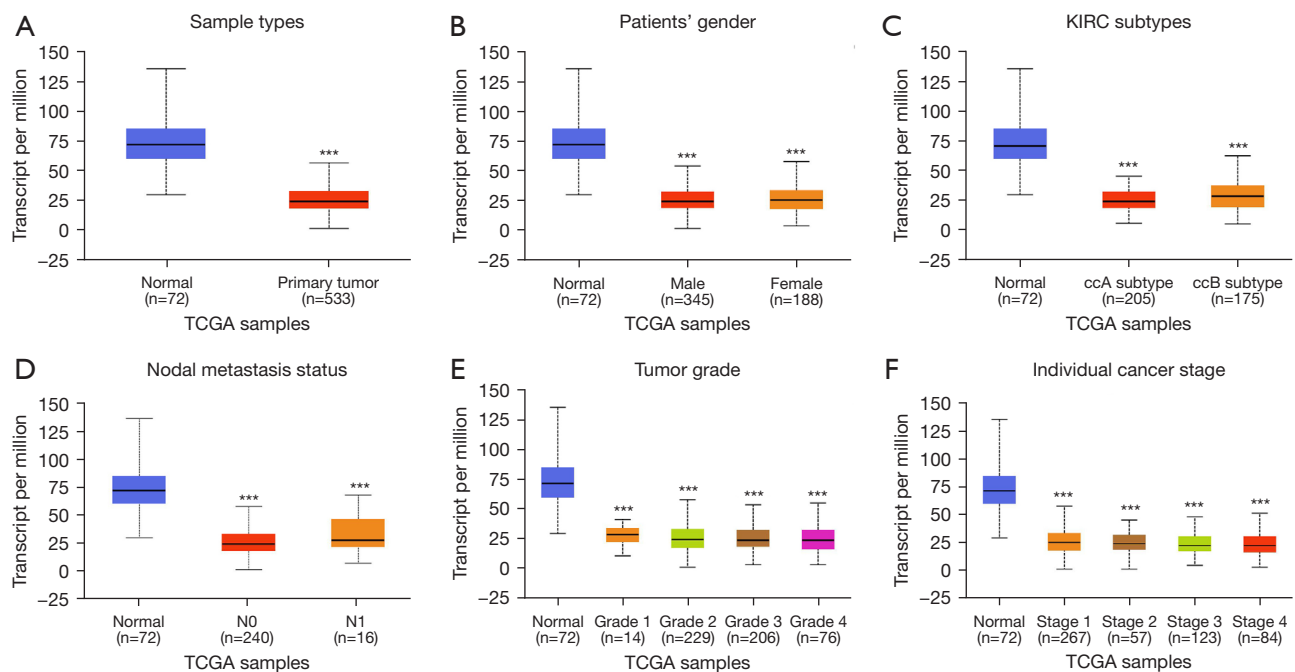


Figure 3 *ACSL4* mRNA expression levels in patients with ccRCC in TCGA dataset cohorts. (A) Plot chart showing the expression of *ACSL4* in ccRCC tissues (n=533) compared with the normal controls (n=72). (B) Plots chart showing *ACSL4* mRNA expression between male and female, (C) KIRC subtypes, (D) between the cases with or without nodal invasion, (E) the cases with different tumor grade and (F) clinical pathological stages. ***, P<0.001. ccRCC, clear cell renal cell carcinoma; TCGA, The Cancer Genome Atlas; KIRC, kidney renal clear cell carcinoma.

observation that inhibiting *ACSL4* expression substantially attenuated cell death caused by erastin (Figure 6B,6C) revealed that *ACSL4* performs an important part in the ferroptosis process. In addition, we examined the degree of iron buildup and lipid peroxidation in RCC4 and A498 cells once the expression of *ACSL4* was silenced using shRNA. After treatment with erastin, the level of lipid ROS was greatly reduced (Figure 6D), but there was no change in the number of accumulated Fe^{2+} (Figure 6E) in RCC4 and A498 cells. We concluded that *ACSL4* might partly participate in ferroptosis by enhancing erastin-mediated lipid peroxidation, mainly because lipid peroxidation is both a defining characteristic of ferroptosis and an inducer of the process.

GO functional annotation and pathway enrichment of *ACSL4*

An investigation into the possible mechanisms of *ACSL4*'s involvement in the malignant bioactivity of KIRC was

carried out by conducting a TCGA-KIRC Gene co-expression network analysis. The cBioPortal of Cancer Genomics was employed in the TCGA-KIRC dataset to determine the highly co-expressed genes with *ACSL4*. A criterion of absolute Spearman's $r \geq 0.5$ was used to identify 295 genes shown to be co-expressed with *ACSL4* (website: <https://cdn.amegroups.com/static/public/tcr-21-2157-01.pdf>). After that, these genes were entered into DAVID so that additional GO analysis and KEGG pathway analysis could be carried out. Figure 7 contains a list of the ten most important terms that were uncovered by the GO and the KEGG analysis. The ubiquitin-mediated proteolysis pathway was shown to be the most substantially enriched for genes co-expressed with *ACSL4* (Figure 7A). In the biological process and molecular function ontology, protein ubiquitination (GO: 0016567) and ubiquitin-protein transferase activity (GO: 0004842) were the primary enriched GO categories (Figure 7B,7C). In the cellular component ontology, the endocytic vesicle (GO: 0030139) is the top category in the pathophysiological process (Figure 7D).

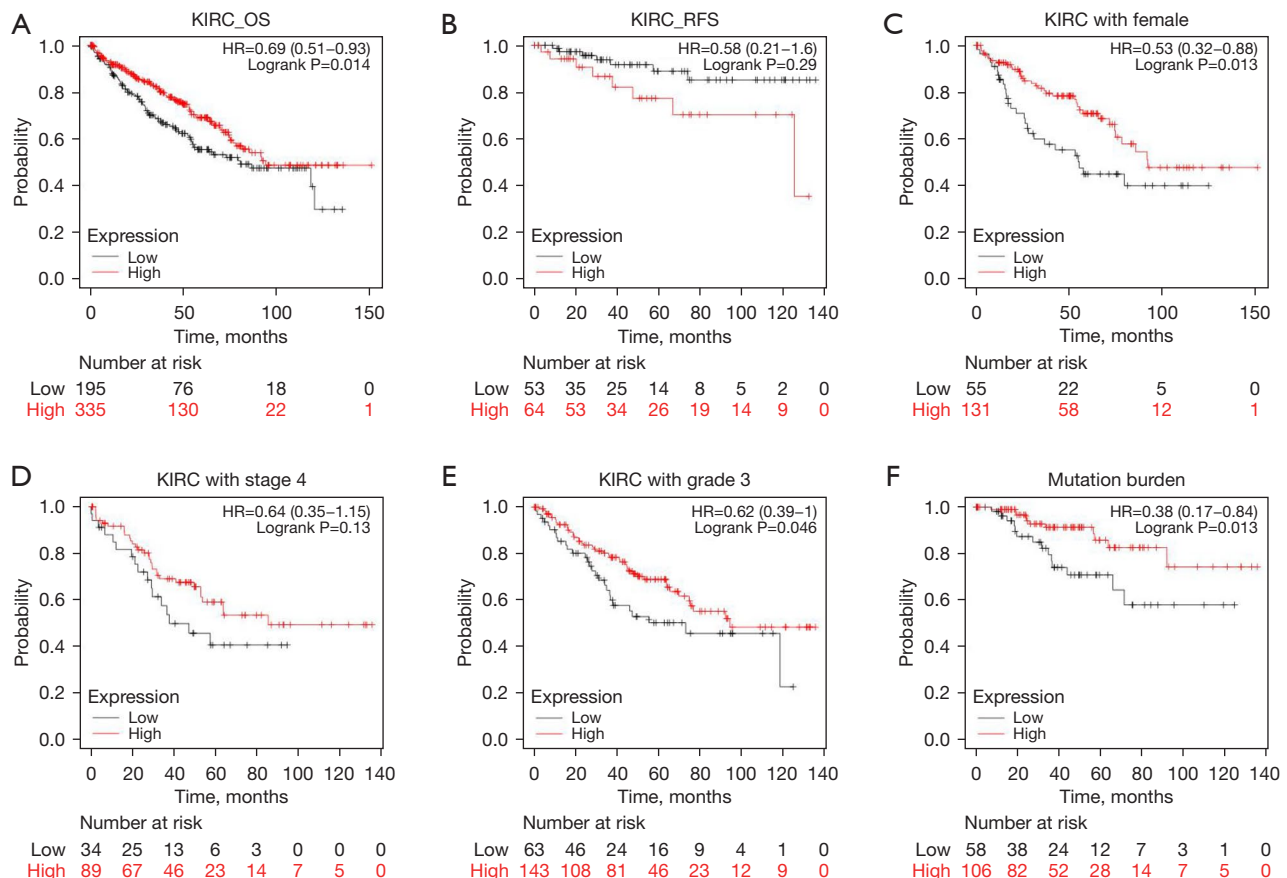


Figure 4 High *ACSL4* expression was associated with favorable survival in patients with ccRCC. (A) Kaplan-Meier curves of OS and (B) RFS in all cases with primary ccRCC. Stratified analysis of OS according to the combination of *ACSL4* and gender (C), tumor stage 4 (D), tumor grade 3 (E), and mutation burden (F), respectively. ccRCC, clear cell renal cell carcinoma; KIRC, kidney renal clear cell carcinoma; OS, overall survival; RFS, recurrence free survival.

Discussion

Ferroptosis was not discovered until 2012 when Dixon *et al.* published their findings on a study they had conducted on a small molecule known as erastin (10). The process of ferroptosis is a novel kind of cell death that is reliant on iron and is linked to oxidative stress (10). Ferroptosis is often hallmarked by an accumulation of cytoplasmic and lipid ROS, a decrease in the volume of the mitochondria, an enhancement in the density of the mitochondrial membrane, the perforation or deletion of mitochondrial cristae, as well as the disintegration of the outer membrane of the mitochondria (19). Recently, it was established that *ACSL4* serves as an important factor of ferroptosis by gene filtering utilizing Genome-Wide CRISPR as well as microarray assessment of anti-ferroptosis cell lines (20). In

the current investigation, the expression profiles of *ACSL4* along with the clinical-pathological characteristics that are linked to ccRCC were analyzed. Furthermore, indicators of ferroptosis such as lipid reactive oxygen species (ROS) and ferric ion (Fe^{2+}) were investigated upon *ACSL4* was dysregulation. As a result, we deduced that the level of *ACSL4* in ccRCC is lower than that in normal tissues, and hypothesized that a lower level of ferroptosis would be linked to the onset and advancement of ccRCC.

According to several research reports, ferroptosis has a very strong correlation with a variety of human disorders (6,7,19). There have only been a few studies done on ferroptosis in relation to ccRCC. Miess *et al.* proposed that decreased metabolism of fatty acids as a result of restriction of beta-oxidation makes renal cancerous cells extremely

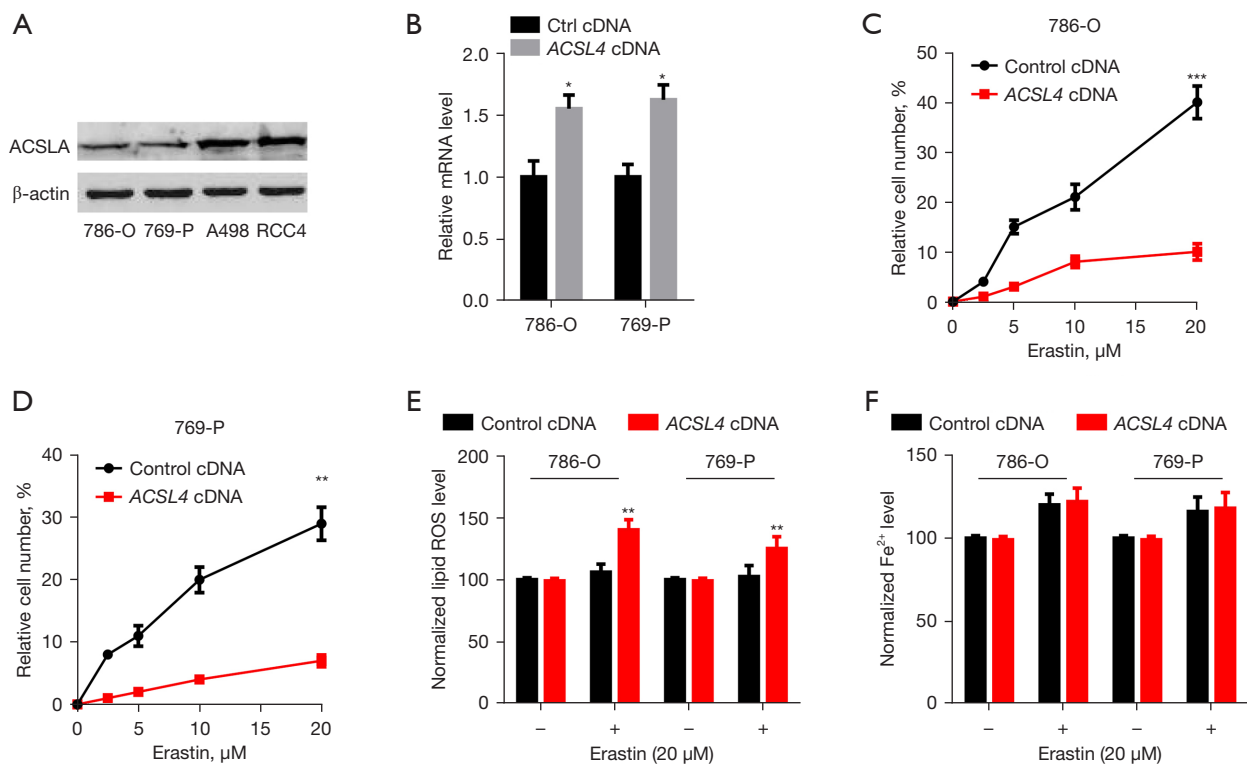


Figure 5 Overexpression of *ACSL4* promotes ferroptosis. (A) Western blot analysis of protein expression of *ACSL4* in indicated cells. (B) *ACSL4* cDNA elevated mRNA expression (*, $P < 0.05$). (C,D) Overexpression of *ACSL4* promoted erastin-induced cell death in 786-O and 769-P cells ($n = 3$, ** $P < 0.01$, *** $P < 0.001$ vs. control cDNA group). (E,F) Lipid ROS and Fe^{2+} were assayed in 786-O and 769-P cells following treatment with erastin for 24 h ($n = 3$, ** $P < 0.01$ vs. control cDNA group). ccRCC, clear cell renal cell carcinoma; ROS, Reactive oxygen species.

reliant on the GSH/GPX pathway to avoid ferroptosis and lipid peroxidation (21). *ACSL4*, in addition to its roles as an important indicator and modulator of ferroptosis, performs an integral function in determining the degree to which ferroptosis is sensitive by altering the cellular lipid content (11). *ACSL4* is responsible for the enrichment of the membrane with the oxidation-prone ω -6 PUFA AA. *ACSL4* is associated and aberrantly regulated in various cancers (4). Recently, the researchers found the level of *ACSL4* expression in RCC cells decreased, whereas raised *ACSL4* levels could promote ferroptosis in RCC cells (12). Consistent with the findings from other studies, we discovered that the expression of *ACSL4* was down-modulated in tumors and that this was linked to an unfavorable prognosis, implying that *ACSL4* might represent a valuable biological marker and a possible treatment target for ccRCC. However, according to the findings of the research conducted by Peng Lee, ectopic *ACSL4* expression in *ACSL4*-negative prostate cancer (PCa) cells contributed to an enhanced capacity of

cells to proliferate, migrate, and invade. On the other hand, deletion of *ACSL4* in PCa cells that express endogenous *ACSL4* results in attenuation in proliferative, migratory, and invasive capacities of cells. They also found that *ACSL4* is responsible for the upregulation of many different pathway proteins, particularly β -catenin, LSD1, and p-AKT (22).

Ferroptosis, like other types of cell death, is intimately linked to particular signaling pathways. The presence of ferroptosis is closely linked to iron buildup and lipid peroxidation as the two most important causal factors (10). An *ACSL4* upregulation plasmid or a silencing plasmid against *ACSL4* was transfected into 4 distinct ccRCC cell lines to confirm the involvement of *ACSL4* in ferroptosis in ccRCC. According to the findings, blocking *ACSL4* may protect cells from death mediated by erastin as well as the generation of lipid ROS. However, the expression of *ACSL4* did not have any effect on the buildup of Fe^{2+} that was induced by erastin. *ACSL4*, which functions as an enzyme that activates fatty acids, preferentially works with long-

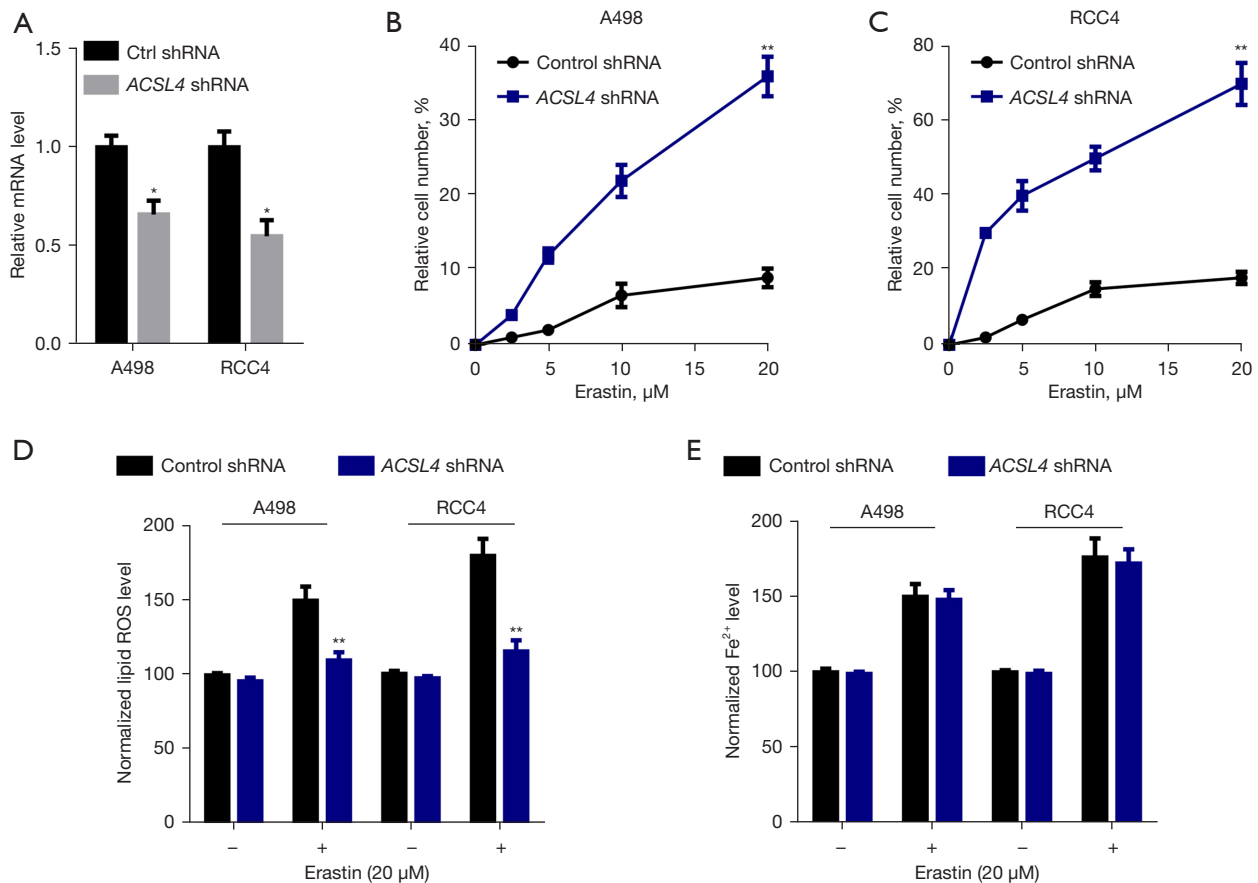


Figure 6 Knockdown of *ACSL4* inhibits ferroptosis. (A) *ACSL4* shRNA decreased mRNA expression (*, $P < 0.05$). (B,C) Knockdown of *ACSL4* inhibited erastin-induced cell death in A498 and RCC4 cells ($n = 3$, **, $P < 0.01$ vs. control shRNA group). (D,E) Lipid ROS and Fe^{2+} were assayed in A498 and RCC4 cells following treatment with erastin for 24 h ($n = 3$, **, $P < 0.01$ vs. control shRNA group).

chain polyunsaturated fatty acids as its substrates. *ACSL4* is responsible for catalyzing the synthesis of these fatty acids as well as the associated coenzyme A (11), thus influencing the process of lipid peroxidation.

Besides investigating the interaction that occurs between ferroptosis and other kinds of cell death, it is pertinent to examine the functionality and assess the molecular and pathway components connected to ferroptosis. Some recently discovered proteins, including metallothionein-1G, NCOA4, and PEBP1 have been linked to ferroptosis via the processes of iron metabolism and lipid peroxidation (23). By applying GO and KEGG, we confirmed that the gene that is co-expressed with *ACSL4* is remarkably enriched in the pathway that is linked to protein ubiquitination. According to the findings of many research reports, the process of ubiquitination has a role in the modulation of the ferroptosis pathway (24). Recent research has shown

that the protein BAP1 reduces the degree of histone 2A ubiquitination affinity to the promoters of the ferroptosis suppressor gene *SLC7A11*, which in turn suppresses the expression of *SLC7A11* in a deubiquitinating-dependent way (25). Additionally, *BAP1* prevents the absorption of cystine by suppressing the expression of *SLC7A11*. This results in an increase in lipid peroxidation as well as ferroptosis. The current work demonstrates that similar to *SLC7A11* ubiquitination, the ubiquitination of *ACSL4* could potentially be engaged in the ferroptosis process, which calls for more investigation on the topic.

Additional research on ferroptosis is required not only to shed light on the molecular basis behind the process but also to open the door to the possibility of developing innovative therapeutic approaches. Sorafenib resistance, for instance, has been found to occur in the treatment of metastatic hepatocellular carcinoma as a consequence of the

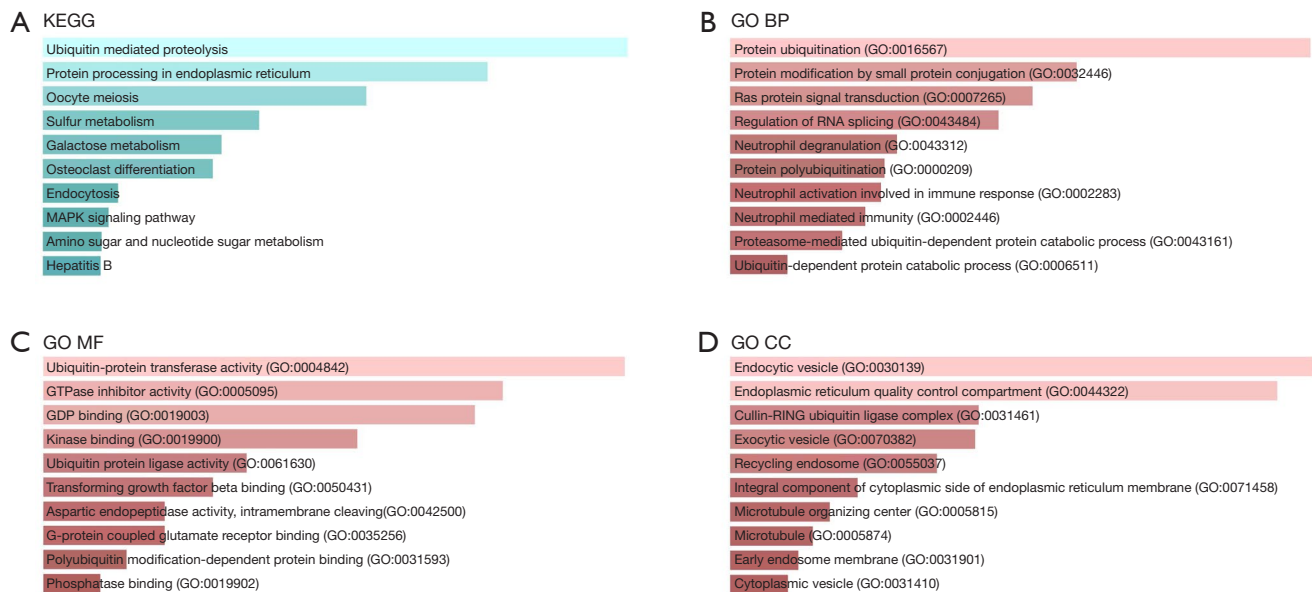


Figure 7 GO and pathway enrichment analysis of the *ACSL4* co-expressed genes in TCGA-KIRC. (A) The most important pathway for gene enrichment of *ACSL4* co-expression was Ubiquitin mediated proteolysis pathway ($P=1.6E-3$). (B,C) In the biological process and molecular function ontology, protein ubiquitination (GO: 0016567; $P=5.0E-4$) and ubiquitin-protein transferase activity (GO: 0004842; $P=1.6E-15$) constituted the majority of enriched GO categories. (D) In the CC ontology, endocytic vesicle (GO: 0030139; $P=6.3E-10$) ranked the top in the pathophysiological process. GO, Gene ontology; KEGG, Kyoto Encyclopedia of Genes and Genomes; BP, biological process; MF, molecular function; CC, cellular component; TCGA, The Cancer Genome Atlas; KIRC, kidney renal clear cell carcinoma.

metallothionein-1G induced suppression of ferroptosis (26). Doll *et al.* additionally showed that pharmacologic targeting of *ACSL4* using the antidiabetic drug family known as thiazolidinediones reduces the degree of tissue death found in a mouse ferroptosis model, indicating that *ACSL4* suppression is a feasible therapeutic strategy for preventing ferroptosis-associated illnesses (20).

Noteworthy shortcomings of our work include the absence of a considerable number of previously analyzed tumor and normal specimens from the database, heterogeneous data, and platform heterogeneity. Furthermore, the majority of the community ethics data in the TCGA database is limited to white and black communities, making it difficult to apply these results to other ethnicities. Prospective research concentrating on the mechanisms of *ACSL4* as predicted by bioinformatics, both *in vivo* and *in vitro*, is warranted to make progress in the field.

Conclusions

Our study demonstrated that *ACSL4* is down-regulated in ccRCC and correlated with patients' clinicopathological

features. *ACSL4* suppresses proliferation of ccRCC cells, at least in part, by activating ferroptosis. These results indicate that *ACSL4* may be regarded as a potential therapeutic target for the treatment of ccRCC and underlie future studies on pathways involving *ACSL4* in a clinical setting.

Acknowledgments

The author thanks Bullet Edits Limited for the linguistic editing and proofreading of the manuscript.

Funding: This study was supported by Guangdong Esophageal Cancer Institute Science and Technology Program (No. Q-201706).

Footnote

Reporting Checklist: The author has completed the REMARK reporting checklist. Available at <https://tcr.amegroups.com/article/view/10.21037/tcr-21-2157/rc>

Conflicts of Interest: The author has completed the ICMJE uniform disclosure form (available at <https://tcr.amegroups.com>).

[com/article/view/10.21037/tcr-21-2157/coif](https://doi.org/10.21037/tcr-21-2157/coif)). The author has no conflicts of interest to declare.

Ethical Statement: The author is accountable for all aspects of the work in ensuring that questions related to the accuracy or integrity of any part of the work are appropriately investigated and resolved. The study was conducted in accordance with the Declaration of Helsinki (as revised in 2013). The study was approved by Academic Committee of Sun Yat-sen University Cancer Center (No. B2018-006-01) and informed consent was taken from all the patients.

Open Access Statement: This is an Open Access article distributed in accordance with the Creative Commons Attribution-NonCommercial-NoDerivs 4.0 International License (CC BY-NC-ND 4.0), which permits the non-commercial replication and distribution of the article with the strict proviso that no changes or edits are made and the original work is properly cited (including links to both the formal publication through the relevant DOI and the license). See: <https://creativecommons.org/licenses/by-nc-nd/4.0/>.

References

- Hsieh JJ, Purdue MP, Signoretti S, et al. Renal cell carcinoma. *Nat Rev Dis Primers* 2017;3:17009.
- Brannon AR, Reddy A, Seiler M, et al. Molecular Stratification of Clear Cell Renal Cell Carcinoma by Consensus Clustering Reveals Distinct Subtypes and Survival Patterns. *Genes Cancer* 2010;1:152-63.
- Farber NJ, Kim CJ, Modi PK, et al. Renal cell carcinoma: the search for a reliable biomarker. *Transl Cancer Res* 2017;6:620-32.
- Kuwata H, Hara S. Role of acyl-CoA synthetase ACSL4 in arachidonic acid metabolism. *Prostaglandins Other Lipid Mediat* 2019;144:106363.
- Orlando UD, Castillo AF, Dattilo MA, et al. Acyl-CoA synthetase-4, a new regulator of mTOR and a potential therapeutic target for enhanced estrogen receptor function in receptor-positive and -negative breast cancer. *Oncotarget* 2015;6:42632-50.
- Sha W, Hu F, Xi Y, et al. Mechanism of Ferroptosis and Its Role in Type 2 Diabetes Mellitus. *J Diabetes Res* 2021;2021:9999612.
- Wang Y, Zhang M, Bi R, et al. ACSL4 deficiency confers protection against ferroptosis-mediated acute kidney injury. *Redox Biol* 2022;51:102262.
- Sha R, Xu Y, Yuan C, et al. Predictive and prognostic impact of ferroptosis-related genes ACSL4 and GPX4 on breast cancer treated with neoadjuvant chemotherapy. *EBioMedicine* 2021;71:103560.
- Mou Y, Wang J, Wu J, et al. Ferroptosis, a new form of cell death: opportunities and challenges in cancer. *J Hematol Oncol* 2019;12:34.
- Dixon SJ, Lemberg KM, Lamprecht MR, et al. Ferroptosis: an iron-dependent form of nonapoptotic cell death. *Cell* 2012;149:1060-72.
- Yuan H, Li X, Zhang X, et al. Identification of ACSL4 as a biomarker and contributor of ferroptosis. *Biochem Biophys Res Commun* 2016;478:1338-43.
- Du Y, Zhao HC, Zhu HC, et al. Ferroptosis is involved in the anti-tumor effect of lycorine in renal cell carcinoma cells. *Oncol Lett* 2021;22:781.
- Rhodes DR, Kalyana-Sundaram S, Mahavisno V, et al. OncoPrint 3.0: genes, pathways, and networks in a collection of 18,000 cancer gene expression profiles. *Neoplasia* 2007;9:166-80.
- Chandrashekar DS, Bashel B, Balasubramanya SAH, et al. UALCAN: A Portal for Facilitating Tumor Subgroup Gene Expression and Survival Analyses. *Neoplasia* 2017;19:649-58.
- Uhlen M, Zhang C, Lee S, et al. A pathology atlas of the human cancer transcriptome. *Science* 2017;357:eaan2507.
- Nagy Á, Munkácsy G, Györffy B. Pancancer survival analysis of cancer hallmark genes. *Sci Rep* 2021;11:6047.
- Gao J, Aksoy BA, Dogrusoz U, et al. Integrative analysis of complex cancer genomics and clinical profiles using the cBioPortal. *Sci Signal* 2013;6:pl1.
- Huang da W, Sherman BT, Lempicki RA. Systematic and integrative analysis of large gene lists using DAVID bioinformatics resources. *Nat Protoc* 2009;4:44-57.
- Peng J, Hao Y, Rao B, et al. A ferroptosis-related lncRNA signature predicts prognosis in ovarian cancer patients. *Transl Cancer Res* 2021;10:4802-16.
- Doll S, Proneth B, Tyurina YY, et al. ACSL4 dictates ferroptosis sensitivity by shaping cellular lipid composition. *Nat Chem Biol* 2017;13:91-8.
- Miess H, Dankworth B, Gouw AM, et al. The glutathione redox system is essential to prevent ferroptosis caused by impaired lipid metabolism in clear cell renal cell carcinoma. *Oncogene* 2018;37:5435-50.
- Wu X, Deng F, Li Y, et al. ACSL4 promotes prostate cancer growth, invasion and hormonal resistance. *Oncotarget* 2015;6:44849-63.

23. Stockwell BR, Friedmann Angeli JP, Bayir H, et al. Ferroptosis: A Regulated Cell Death Nexus Linking Metabolism, Redox Biology, and Disease. *Cell* 2017;171:273-85.
24. Wang X, Wang Y, Li Z, et al. Regulation of Ferroptosis Pathway by Ubiquitination. *Front Cell Dev Biol* 2021;9:699304.
25. Zhang Y, Shi J, Liu X, et al. BAP1 links metabolic regulation of ferroptosis to tumour suppression. *Nat Cell Biol* 2018;20:1181-92.
26. Chen X, Kang R, Kroemer G, et al. Broadening horizons: the role of ferroptosis in cancer. *Nat Rev Clin Oncol* 2021;18:280-96.

Cite this article as: Guo N. Identification of *ACSL4* as a biomarker and contributor of ferroptosis in clear cell renal cell carcinoma. *Transl Cancer Res* 2022;11(8):2688-2699. doi: 10.21037/tcr-21-2157